

## Optical coherence tomography as a novel tool for non-destructive measurement of the hull thickness of lupin seeds

J. C. CLEMENTS<sup>1</sup>, A. V. ZVYAGIN<sup>2</sup>, K. K. M. B. D. SILVA<sup>2</sup>, T. WANNER<sup>2</sup>, D. D. SAMPSON<sup>2</sup>  
and W. A. COWLING<sup>3</sup>

<sup>1</sup> Centre for Legumes in Mediterranean Agriculture, E-mail: clem@cyllene.uwa.edu.au; <sup>2</sup> Optical and Biomedical Engineering Laboratory, Department of Electrical and Electronic Engineering and <sup>3</sup> School of Plant Biology, The University of Western Australia, 35 Stirling Hwy, Crawley, WA 6009, Australia

With 4 figures and 2 tables

Received June 10, 2003/Accepted February 4, 2004

Communicated by W. Swiecicki

### Abstract

Hull thickness is an important component of seed quality, which affects dehulling ability, feed or food nutritional aspects and cooking times. A breeding objective in *Lupinus angustifolius* crop improvement is to reduce hull thickness and a rapid screening method is needed to efficiently screen genotypes. Optical coherence tomography (OCT) imaging using infrared illumination at 980 nm was used to compare hull thickness of genotypes of four lupin species. OCT-derived hull layer thickness correlated highly with actual hull thickness determined by environmental scanning electron microscopy ( $r = 0.90$ ) and allowed reliable distinction between mutant (thin-hulled) and parent genotypes of *L. angustifolius*. The imaging could clearly penetrate lupin seed to a depth of approximately 200  $\mu\text{m}$ . The use of OCT to measure hull thickness has the advantage that it is rapid and non-destructive and should be very useful in selecting thin hull lines of lupins and other species on a single seed basis in germplasm or progeny from crosses.

**Key words:** *Lupinus* — hull — optical coherence tomography — scanning electron microscopy — seed coat testa — seed quality

Crop improvement is becoming increasingly concerned with seed quality aspects such as protein, oil content, anti-nutritional compounds and constituents that influence processing (Basra 1995, Moore and Yaklich 2000). For both cereals and legumes, hull thickness and proportion of seed weight are important for ease of dehulling and food processing, reduced fibre content (and consequently higher oil and protein) and reduced cooking times. Lush and Evans (1980) suggested that selection for reduced hull content has occurred over the millennia in the major pulse crops, with the exception of lupins.

Natural genetic variability for hull proportion and thickness occurs in several legume species, e.g. for pea (Ali Khan 1993), common bean (*Phaseolus vulgaris*, Escribano et al. 1997), chickpea (Waldia et al. 1996) and lupin (Reader and Dracup 1998, Clements and Dracup 2001, Clements et al. 2002). Of the agriculturally important lupin species, both *Lupinus angustifolius* and *L. luteus* have a high percentage of seed weight in the hull (24 and 25%, respectively) (Lush and Evans 1980, Reader and Dracup 1998, Clements et al. 2002) compared with only 7% in soybean (Lush and Evans 1980) and 9% in field pea (Ali Khan 1993).

*Lupinus angustifolius* has a relatively low metabolizable energy content for pig and poultry as a consequence of its high

percentage of hull. The hull consists of cellulose (50%), hemicelluloses and pectins (Brillouet and Riochet 1983). The kernel is also high in non-starch polysaccharides within the cell walls and oligosaccharides that constitute approximately 30% and 10%, respectively, of the dehulled kernel (Brillouet and Riochet 1983, Evans 1994). De-hulling lupins improves nutritive value for monogastric animals such as pigs, poultry and fish species (Edwards and Barneveld 1998) but the cost of this process tends to make it uneconomical. Significant genetic variation occurs for hull proportion in *L. angustifolius* (Clements et al. 2002) and breeding for reduced hull content has the potential to increase metabolizable energy, protein or oil (Stombaugh et al. 2000, Clements et al. 2002), harvest index and yield.

A rapid method for screening germplasm would be preferred for selecting new lines with reduced hull content. Methods for estimating hull proportion range from manual removal and weighing (Black et al. 1998a, Clements et al. 2002) to the use of dehulling devices (Black et al. 1998b). Flinn et al. (1998) investigated the use of near-infrared spectroscopy for food processing characteristics of field pea and chickpea, and further development of the method is necessary. Several technologies that allow *in vivo* imaging of plant tissues such as magnetic resonance imaging (Faust et al. 1997) and confocal microscopy (Running et al. 1995) have been limited by factors such as low resolution, long acquisition time and limited penetration, respectively. Optical coherence tomography (OCT) is a relatively new imaging technique (Huang et al. 1991, Masters 1999) that has shown significant promise in the micron-resolution subsurface imaging of semitransparent and turbid media. Most research in OCT has focussed on *in vivo* imaging of tissues such as the eye, the skin, and the superficial layers of internal hollow organs. However, OCT has recently been adapted to imaging of living plant tissues (Hettinger et al. 2000). OCT provides a unique set of capabilities, including: (i) greater penetration than confocal microscopy; (ii) resolution typically in the 10 micron range; (iii) video-rate image acquisition; and (iv) portability. Such capabilities make it a potentially useful tool in seed hull screening. In this paper, the utility of OCT for rapid, non-destructive screening for reduced seed hull thickness of lupins is demonstrated.

## Materials and Methods

**Plant materials:** Homogeneous seed of two genotypes of *L. angustifolius*, 83A:473 (parent genotype) and 11257 (mutant genotype), and three other species (*L. albus* cv. 'Kiev', *L. luteus* cv. 'Wodjil', *L. mutabilis*, accession P27033) were sourced from bulks grown in a greenhouse at the University of Western Australia Field Station, Shenton Park in 1999. 83A:473 is an advanced breeding line from the Western Australian Department of Agriculture lupin breeding programme and 11257 is a thin hull mutant line selected as a single M<sub>3</sub> plant from ethyl methane sulphonate-treated 83A:473 (Clements and Dracup 2001). The mutant line was found to have a 23% reduction in thickness of hull (Clements and Dracup 2001). Fifteen randomly selected seeds of 83A:473 and mutant (11257), respectively, were individually labelled and subjected to OCT imaging and scanning electron microscopy (SEM). Smaller seed samples of the other three species were also included to test the application of the methods to seed types of differing hull thickness and structure.

**OCT imaging:** The imaging was performed using an OCT system built in house and shown schematically in Fig. 1. The key subsystem is a Michelson interferometer in which light is split into two paths. One path, known as the reference path, is terminated by a reflective scanning optical delay line, which is used to vary the path length. The other path is terminated by the sample, which here is a seed. A low-power, infrared light source with a broad optical bandwidth is used. A broad optical bandwidth ensures that coherent interference takes place at the output of the interferometer only when the two paths are matched in length to within several coherence lengths,  $l_c$ . The coherence length is related to the optical bandwidth by Huang et al. (1991)

$$l_c = \frac{2 \ln(2) \lambda_0^2}{\pi \Delta \lambda}$$

where,  $\lambda_0$  is the mean wavelength,  $\Delta \lambda$  is the bandwidth, and a Gaussian spectral profile has been assumed. The signature of coherent interference is the presence of interference fringes which, in turn, signify that a reflection exists in the sample. Following photodetection, the envelope of the interferogram is extracted using an analogue circuit, then digitized and transferred to computer for display and storage.

The OCT system records the envelope of the interferogram as the reference path is scanned, thus, providing an axial profile of reflectivity vs. optical length. The optical length is  $n_s$  times greater than the associated physical length, where  $n_s$  is the refractive index of

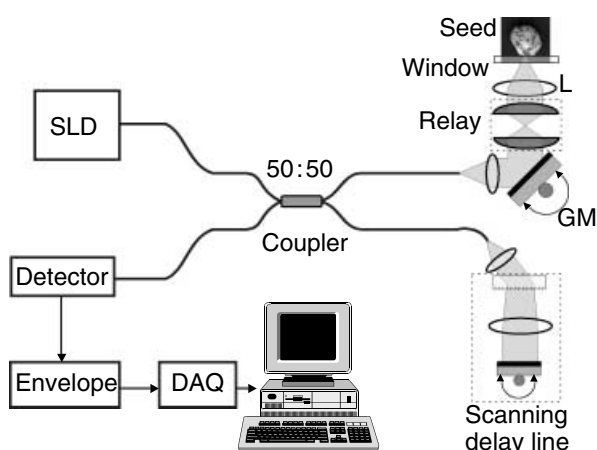


Fig. 1: Schematic diagram of optical coherence tomography set-up. SLD, superluminescent diode; L, lens; GM, galvanometer mirror; DAQ, data acquisition card

the sample. Simultaneously with the axial scan, the beam is rastered across the sample using a galvanometer-mounted mirror (GM) and lens assembly, such that a tomograph of the reflectivity profile of a sample is built up. The transverse resolution of the system,  $l_{\text{trans}}$ , is given by

$$l_{\text{trans}} = \frac{4\lambda_0 f}{\pi d}$$

where,  $d$  is the beam diameter at the lens (L) of focal length  $f$ .

For the OCT system here, a superluminescent diode source with mean wavelength  $\lambda_0 = 977$  nm and optical bandwidth,  $\Delta \lambda = 24$  nm, is used and the interferometer is implemented using single-mode optical fibre and a 50/50 fibre coupler. The scanning delay line employs a frequency-domain diffraction grating/tilt mirror optical circuit (Rollins et al. 1998). The measured axial resolution is  $24 \mu\text{m}$  and the transverse resolution is estimated to be  $l_{\text{trans}} = 30 \mu\text{m}$ . The OCT system acquires frames comprising  $128 \times 256$  pixels at the rate of 4/s, with corresponding dimensions of approximately  $1000 \times 800 \mu\text{m}$  in the lateral and axial directions, respectively, where the axial dimension is measured in terms of optical length. The incident power at the surface of the seed was estimated to be  $< 1$  mW, which is estimated to be well within safe limits according to the Australian/New Zealand Standard, AS/NZS 2211:1997.

**Image processing procedure:** To obtain a cross-sectional image, the seed under test was placed on a flat optical window and oriented manually such that the transverse scan was aligned perpendicular to the funiculus-hilum embryo axis.

For each seed, 12 frames were recorded and averaged to form an image. An automated routine was used to obtain a quantitative measure of cell layer thickness from the recorded images. The automated routine first corrects for the curvature of the layers by averaging all axial line scans to produce average profiles in each of 12 zones. Trial and error was used to determine that 12 zones were sufficient. The average profiles of each zone are then aligned and averaged to yield an averaged hull profile. In order to convert optical length measured using OCT to physical length, a refractive index of  $n_s = 1.5$  is assumed. On average, the entire measurement procedure takes approximately 30 s per seed. Manual positioning of a seed is the most time-consuming part of the procedure. The frame capture and automated measurement routine require approximately 3 and 5 s, respectively.

**Light microscopy:** To examine the tissue structure of both thin-hulled mutant and parent hulls, segments of hull were fixed in 4% glutaraldehyde, dehydrated in a graded alcohol series, and embedded in glycol methacrylate (Feder and O'Brien 1968). Sections ( $2 \mu\text{m}$  thick) were stained with 0.5% toluidine blue (pH 4.0). Sections prepared in this way are thicker as a result of hydration compared with SEM images.

**Scanning electron microscopy:** The same seeds of each line that were scanned with OCT were dissected at the point of OCT scanning and portions of hull mounted for examination under an Electroscan environmental SEM (E-3, 1991) equipped with LINK Si(Li) PCXA EDS (1991), BSED and CL detectors, a UWA/Peltier cold stage and a PC-based digital image capturing system (Image Slave, MEECO Holdings Pty Ltd, North Parramatta, Australia) that allowed examination of uncoated material under hydrous conditions. Samples were imaged at 260 Pa chamber pressure using 30 KeV beam energy,  $40 \mu\text{m}$  spot size and a working distance of 8.0 mm. A copper grid of known dimensions was used to verify the accuracy of the scale bar imprinted on the images generated. For each seed, the thickness of the hull (from epidermis to endodermis), was measured at three locations  $150 \mu\text{m}$  apart on the SEM images and the average thickness calculated. Additionally, after examination of OCT images, measurements were also obtained from the SEM images for layers of cells as described in the Results section.

## Results

Radial light microscopy and SEM sections through the hull of *L. angustifolius* parent and mutant genotypes are shown in Fig. 2a and b. Figure 2c shows OCT images representing radial scans through the seed hull of size approximately  $1000 \times 530 \mu\text{m}$  in the lateral and axial directions, respectively. OCT images show two layers, which correspond to the two layers of palisade cells and the layer of hour-glass cells. After comparison with SEM images, two layers were defined. Layer 1 extends from the epidermis to the base of the first layer of columnar palisade cells. Layer 2 extends from the base of layer 1 to the base of the hour-glass cell layer. These layers are indicated in Fig. 2.

Figure 3 shows a representative OCT image and corresponding hull profile of the mutant lupin genotype. The first peak (labelled '1') corresponds to the interface between the glass optical window and air. The width of the peak is  $24 \mu\text{m}$  and is a measure of the axial resolution of the OCT system. The morphological features evident in Fig. 3 were typically prominent in OCT images of both parent and mutant genotypes. The second peak (labelled '2') in Fig. 3 indicates the air/palisade cell layer interface, which is followed by a layer characterized by no detectable back-scattered signal. No detectable signal identifies this layer (layer 1) as an optically dense and uniform medium. Layer 2 extends from the location labelled '3' in Fig. 3b to the fourth peak (labelled '4'). Layer 2 is defined from the onset of the detectable signal to the third peak and is associated with the second palisade cell layer (cf.

Fig. 2a and b). The third peak (between positions labelled '3' and '4') arises from the interface between the palisade cell layer and the hour-glass cell layer. As seen in Fig. 3, this peak is of greater width than expected based on the axial resolution of OCT, and we believe its width is correlated with the thickness of the hour-glass cell layer. This broad peak indicates that there is a large contrast in density and possibly various structural differences, such as lignification and cellulose secondary thickening, between these two tissue types. An OCT-derived measurement for the entire hull could not be made because the interface between hull endodermis and kernel surface cells could not be distinguished in the OCT image.

Based on SEM-determined measurements, the *L. angustifolius* test genotypes, mutant and parent, were found to differ for depth of layer 2, the sum of layers 1 and 2 and entire hull thickness ( $P < 0.001$ ) but were not significantly different for depth of layer 1 (Table 1). Based on OCT-derived values, mutant and parent differed for layer 1, layer 2, and the sum of layers 1 and 2. OCT-derived values for layer 2 were more discriminating between mutant and parent than for layer 1.

Inclusion of *L. luteus*, *L. albus* and *L. mutabilis* widened the range of hull thicknesses to be investigated from 98 (*L. mutabilis*) to  $197 \mu\text{m}$  (parent mean, *L. angustifolius*). Correlations between SEM-derived values of hull layer thickness or entire hull thickness and OCT-derived values for layers 1 and 2 determined across all four species are shown in Table 2. There is a strong correlation between SEM layer 2

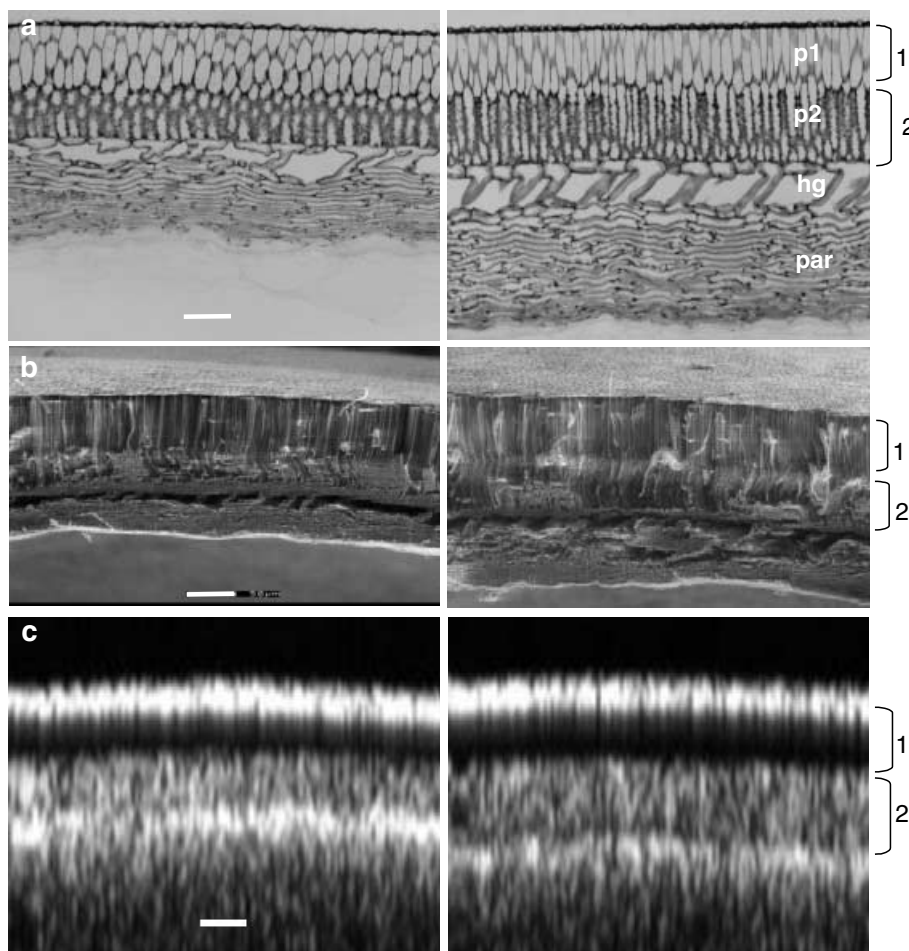


Fig. 2: Cross-sectional images of *Lupinus angustifolius* mutant (left) and parent (right) genotypes obtained using: (a) light microscopy; (b) environmental scanning electron microscopy; and (c) optical coherence tomography. p1, first palisade layer; p2, second palisade layer; hg, hour-glass cell layer; par, parenchymatous layer. OCT-derived cell layers are indicated as '1' and '2'. Scale bars are  $50 \mu\text{m}$

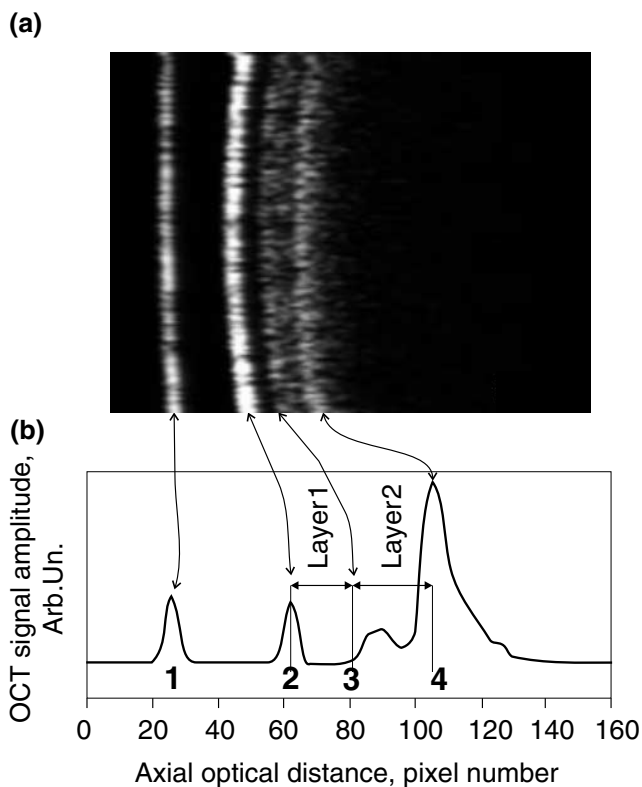


Fig. 3: (a) An optical coherence tomography (OCT) image, and (b) the corresponding hull profile of a mutant seed hull. The correspondence between layer interfaces in (a) and transition points in (b) is shown by arrows. The interfaces labelled by numbers in (b) correspond to: (1) glass/air; (2) air/first palisade cell layer; (3) first palisade cell layer/second palisade cell layer; and (4) second palisade cell layer/hour-glass cell layer

Table 1: Descriptive statistics for SEM and OCT-derived measurements ( $\mu\text{m}$ ) of layers 1, 2 and entire hull for mutant and parent genotypes [n = 13 (mutant), 15 (parent)]

	Mutant		Parent		LSD (0.05)	t-Test
	Mean	SD	Mean	SD		
SEM layer 1	57.2	5.8	59.7	4.5	3.9	NS
SEM layer 2	43.6	4.4	62.9	7.6	4.8	*
SEM entire hull	144.4	12.0	196.9	20.0	12.6	*
OCT layer 1	55.0	2.9	65.5	3.3	2.3	*
OCT layer 2	68.0	3.8	106.5	9.6	5.6	*
OCT layers 1 + 2	122.9	4.3	172.0	10.8	6.3	*

SEM, scanning electron microscopy; OCT, optical coherence tomography; NS, not significant; \* significant at P = 0.001.

Table 2: Pearson correlation coefficients (r) and probability values (indicated by asterisks) for SEM and OCT-derived measurements of entire hull thickness and hull layers (layers 1 and 2; n = 28)

	SEM layer 1	SEM layer 2	SEM layers 1 + 2	SEM entire hull	OCT layer 1	OCT layer 2
SEM layer 1	1.00					
SEM layer 2	0.52**	1.00				
SEM layers 1 + 2	0.78***	0.94***	1.00			
SEM entire hull	0.58***	0.96***	0.93***	1.00		
OCT layer 1	0.42*	0.62***	0.62***	0.64***	1.00	
OCT layer 2	0.41*	0.87***	0.80***	0.87***	0.48**	1.00
OCT layers 1 + 2	0.45**	0.90***	0.84***	0.90***	0.65***	0.98***

\*, \*\*, \*\*\*Significant at P = 0.05; P = 0.01; and P = 0.001 respectively. SEM, scanning electron microscopy; OCT, optical coherence tomography.

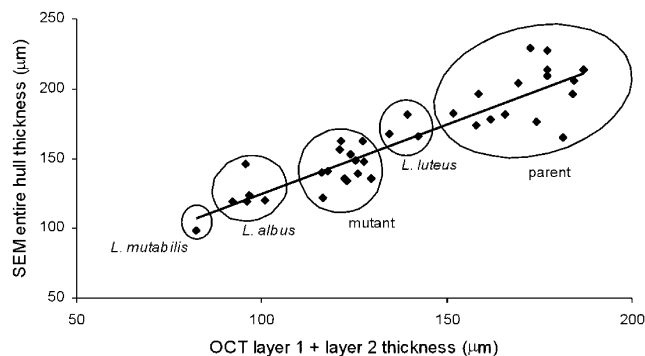


Fig. 4: Relationship between scanning electron microscopy (SEM)-derived values for entire hull thickness and optical coherence tomography (OCT)-derived sum of layers 1 and 2 for five lupin genotypes: *Lupinus angustifolius* parent and thin-hulled mutant, *L. luteus* cv. ‘Wodjil’, *L. albus* cv. ‘Kiev’, and *L. mutabilis* accession P27033. The solid line is a least-squares fit to the data,  $r = 0.90$

and OCT layer 2 ( $r = 0.87$ ) but a lower correlation between SEM layer 1 and OCT layer 1 ( $r = 0.42$ ) values. The highest correlations for entire hull thickness between SEM and OCT data is obtained for OCT sum of layers 1 and 2 ( $r = 0.90$ ,  $y = 0.99x + 26.0$ , Fig. 4) and OCT layer 2 only ( $r = 0.87$ ). The relationship between entire hull thickness and OCT layers 1 and 2, shown in Fig. 4, can be used to predict actual hull thickness for individual seeds in test batches using only OCT data. Light microscopy images revealed that in *L. mutabilis*, which had the thinnest seed coat of the four lupin species studied, there is only one layer of columnar palisade cells between the epidermis and the hour-glass layer. This agrees very well with the undetectable signal layer 2 using OCT.

### Discussion

The measurement of optical thickness of layers, rather than their true physical thickness, implies a potential uncertainty in using OCT for layer thickness determination. In the current study, as stated, a value for the refractive index of seed hull was assumed as  $n_s = 1.5$ . However, it is also possible to employ a slightly modified apparatus capable of determining the refractive index and, thus, rendering absolute accuracy to thickness measurements (Knüttel and Behlau-Godau 2000). However, as discussed below, such improvements may not be required.

Lush and Evans (1980) have described the anatomy of the hull of several lupin species. Lupin species vary in the overall thickness, surface morphology and ratios of thickness among

the cell layers that make up the hull. Within species such as *L. angustifolius*, enough variation exists either in wild, semi-domesticated or in breeding line germplasm or in mutation populations to prompt the search for rapid screening tools to efficiently identify genotypes with the desired hull properties (Reader and Dracup 1998). Hull proportion data derived from weights of separated hulls and kernels has been used as a surrogate for hull thickness when screening germplasm of lupins (Clements et al. 2002) and chickpea (Waldia et al. 1996) but it has the disadvantage of being tedious and its reflection of true hull thickness is confounded by variation in seed size.

The use of OCT to measure hull thickness has advantages in that it is rapid and non-destructive. Without automation of sample placement and data capture, it is expected that seeds could be processed at a rate exceeding 100/h. The data presented here show that it was possible to produce values of hull layers that correlate well with actual entire hull thickness, although it was not possible to directly measure the entire hull thickness with OCT. Both the sum of OCT-derived layers 1 and 2 or OCT-derived layer 2 only could reliably be used to predict actual hull thickness (Fig. 4) and seed of a thin hulled mutant could be distinguished from the normal hulled parent type. Different species of lupins could also be distinguished. The regression line of hull thickness as predicted by OCT layers 1 + 2 explained 81% of the variation observed in hull thickness determined by SEM. It is expected that OCT will be very useful in screening for thin hull lines in germplasm or progeny from crosses on a single seed basis. Selection of single seeds for hull thickness by OCT will allow selection before sowing, rather than on harvested seed as with current measurements. This is more efficient and will accelerate the breeding process.

Based on published reports of the structure and existence of cell layers of hulls of other species (Lush and Evans 1980), this method should apply to a range of crops. It could facilitate plant breeding programmes that are selecting for seed quality improvements through altered hull thickness such as in the lupin breeding programme in Western Australia or in other programmes interested in hull properties in relation to quality characteristics (Hung et al. 1993, Waldia et al. 1996).

#### Acknowledgements

The authors acknowledge Ms Sharon Platten (Centre for Microscopy and Microanalysis, University of Western Australia) for assistance with electron microscopy, and Mr J. FitzGerald for his contribution at the initial stages of this work.

#### References

- Ali Khan, S. T., 1993: Seed hull content in field pea. *Can. J. Plant Sci.* **73**, 611–613.
- Basra, A. S., 1995: *Seed Quality: Basic Mechanisms and Agricultural Implications*. Food Products Press, New York.
- Black, R. G., J. B. Brouwer, C. Meares, and L. Iyer, 1998a: Variation in physico-chemical properties of field peas (*Pisum sativum*). *Food Res. Int.* **31**, 81–86.
- Black, R. G., U. Singh, and C. Meares, 1998b: Effect of genotype and pre-treatment of fieldpeas (*Pisum sativum*) on their dehulling and cooking quality. *J. Sci. Food Agric.* **77**, 251–258.
- Brillouet, J. M., and D. Riochet, 1983: Cell wall polysaccharides and lignin in cotyledons and hulls of seeds from various lupin (*Lupinus L.*) species. *J. Sci. Food Agric.* **34**, 861–868.
- Clements, J. C., and M. Dracup, 2001: Lowering the seed hull proportion in narrow-leaved lupin (*L. angustifolius*). *Proc. of the Fourth Europ. Conf. Grain Legumes*, Cracow, Poland, 293.
- Clements, J. C., M. Dracup, and N. Galwey, 2002: Effect of genotype and environment on proportion of seed hull and pod wall in narrow-leaved lupin (*Lupinus angustifolius L.*). *Aust. J. Agric. Res.* **53**, 1147–1154.
- Edwards, A. C., and R. J. Barneveld, 1998: Lupins for livestock and fish. In: J. S. Gladstones, C. A. Atkins, and J. Hamblin (eds), *Lupins as Crop Plants: Biology, Production and Utilization*, 385–410. CAB International, Oxon, UK.
- Escribano, M. R., M. Santalla, and A. M. de Ron, 1997: Genetic diversity in pod and seed quality traits of common bean populations from north-western Spain. *Euphytica* **93**, 71–81.
- Evans, A. J., 1994: The carbohydrates of lupins, composition and uses. In: M. Dracup, and J. Palta (eds), *Proceeding of First Australian Lupin Technical Symposium*, 110–114. Western Australian Department of Agriculture, South Perth.
- Faust, M., P. C. Wang, and J. Maas, 1997: The use of magnetic resonance imaging in plant science. *Hort. Rev.* **20**, 225–266.
- Feder, N., and T. P. O'Brien, 1968: Plant microtechnique: some principals and new methods. *Am. J. Bot.* **55**, 123–142.
- Flinn, P. C., R. G. Black, L. Iyer, J. B. Brouwer, and C. Meares, 1998: Estimating the food processing characteristics of pulses by near infrared spectroscopy, using ground or whole samples. *J. Near Infrared Spectrosc.* **6**, 213–220.
- Hettinger, J. W., M. de la PeñaMattozzi, W. R. Myers, M. E. Williams, A. Reeves, R. L. Parsons, R. C. Haskell, D. C. Petersen, R. Wang, and J. I. Medford, 2000: Optical coherence microscopy. A technology for rapid, in vivo, non-destructive visualization of plants and plant cells. *Plant Physiol.* **123**, 3–15.
- Huang, D., E. A. Swanson, C. P. Lin, J. S. Schuman, W. G. Stinson, W. Chang, M. R. Hee, T. Flotte, K. Gregory, C. A. Puliafito, and J. G. Fujimoto, 1991: Optical coherence tomography. *Science* **254**, 1178–1181.
- Hung, T. V., L. H. Liu, R. G. Black, and M. A. Trehwella, 1993: Water absorption in chickpea (*Cicer arietinum*) and field pea (*Pisum sativum*) cultivars using the Peleg model. *J. Food Sci.* **58**, 848–852.
- Knüttel, A., and M. Behlau-Godau, 2000: Spatially confined and temporally resolved refractive index and scattering evaluation in human skin performed with optical coherence tomography. *J. Biomed. Opt.* **5**, 83–92.
- Lush, W. M., and T. Evans, 1980: The seed coats of cowpeas and other grain legumes: structure in relation to function. *Field Crops Res.* **3**, 267–286.
- Masters, B. R., 1999: Early development of optical low-coherence reflectometry and some recent biomedical applications. *J. Biomed. Opt.* **4**, 236–247.
- Moore, S. H., and R. W. Yaklich, 2000: Genetic improvement of seed quality. *Proc. Symposium Sponsored by Divisions C-4, C-1, and C-8 of the Crops Science Society of America in Anaheim, CA*, 29 October, 1997.
- Reader, M., and M. Dracup, 1998: Hull and Pod Wall Weights in Lupin. *Crop Updates 1998*. Western Australian Department of Agriculture, Perth, Western Australia.
- Rollins, A. M., M. D. Kulkarni, S. Yazdanfar, R. Ung-Arunyawee, and J. A. Izatt, 1998: In vivo video rate optical coherence tomography. *Opt. Expr.* **3**, 219–229.
- Running, M. P., S. E. Clark, and E. M. Meyerowitz, 1995: Confocal microscopy of the shoot apex. *Methods Cell Biol.* **49**, 217–229.
- Stombaugh, S. K., H. G. Jung, J. H. Orf, and D. A. Somers, 2000: Genotypic and environmental variation in soybean seed cell wall polysaccharides. *Crop Sci.* **40**, 408–412.
- Waldia, R. S., V. P. Singh, D. R. Sood, P. K. Sardana, and I. S. Mehla, 1996: Association and variation among cooking quality traits in Kabuli chickpea (*Cicer arietinum L.*). *J. Food Sci. Technol.* **33**, 397–402.